X-ray Structures and Complete NMR Assignment by DFT Calculations of $[Os(bpy)_2(CO)Cl]PF_6$ and $[Os(bpy)_2(CO)H]PF_6$ Complexes

Roberto Gobetto,* Carlo Nervi, Barbara Romanin, and Luca Salassa

Dipartimento di Chimica IFM, Università di Torino, Via P. Giuria 7, 10125 Torino, Italy

Marco Milanesio and Gianluca Croce

Dipartimento di Scienze e Tecnologie Avanzate, Università del Piemonte Orientale "A. Avogadro", Corso T. Borsalino 54, 15100 Alessandria, Italy

Received April 29, 2003

The X-ray structures of $[Os(bpy)_2(CO)(Cl)][(PF_6)]$ (**1**) and $[Os(bpy)_2(CO)(H)][(PF_6)]$ (**2**) (where bpy = 2,2′-bipyridine) have been solved. In complex **1**, belonging to the *C*2/*c* space group, the Cl^- and CO ligands are statically disordered along two almost orthogonal directions, and this disorder may be explained by the steric similarity of the CO and Cl^- groups. Conversely, in complex **2**, the CO and hydride ligands are rather different and the $[Os(bpy)_2(CO)(H)]$ moiety does not show any disorder. A more accurate model of the disordered structure of complex **1** and the hydride position in complex **2** were obtained by DFT calculations. Complete ^1H NMR chemical shift assignments were made, using 1D and 2D NMR experiments combined with theoretical calculations. The experimental ^1H NMR data have been fully interpreted with the aid of magnetic shielding constant calculations, by means of the GIAO (gauge-including atomic orbitals) method, carried out at the B3LYP level. Proton nuclear shielding constants have been calculated with the 6-311G++(2d) basis set, and geometry optimizations have been carried out employing the LanL2Dz basis set for osmium and the 3-21G or 6-31G(d) basis sets for the other atoms. Calculated and experimental results have been compared with a satisfactory level of agreement. The complete assignment of the proton spectrum of **2**, in good agreement with the theoretical data, was confirmed by the $^1H-^1H$ NOESY results. By using this mixed experimental and theoretical approach it was also possible to obtain a calculated structure and the ^1H NMR assignment of $[Os(bpy)_2(CO)(CF_3SO_3)][(CF_3SO_3)]$ (**3**), for which no suitable crystal could be obtained.

Introduction

During the past decade there has been extensive interest in the area of polypyridine complexes of transition metals, especially ruthenium.[1,2] These complexes display peculiar photochemical and photophysical properties, and it is not surprising that the number of their applications in many technological fields is rapidly growing.[3−6] They have been successfully applied in electron transfer processes[7−11] and as catalytic and stoichiometric redox reagents.[12,13] Their luminescent properties have also found applications in solar energy converters,[14] in electroluminescent systems,[15] and, particularly, in probes and sensors.[16,17] In the literature, a large number of crystal structures of $Ru(bpy)_2$ derivatives (where bpy = 2,2′-bipyridine) have been reported, but the number of $Os(bpy)_2$ structures is still quite limited.[18−27] Only three crystal structures containing

(1) Kaes, C.; Katz, A.; Hasseini, M. W. *Chem. Rev.* **2000**, *100*, 3553.
(2) Venturi, M.; Credi, A.; Balzani, V. *Coord. Chem. Rev.* **1999**, *186*, 233.
(3) Piguet, C.; Bernardinelli, G.; Hopfgartner, G. *Chem. Rev.* **1997**, *97*, 2005.
(4) Knof, U.; von Zelewsky, A. *Angew. Chem., Int. Ed.* **1999**, *38*, 303.
(5) Kalyanasundaram, K.; Grätzel, M. *Coord. Chem. Rev.* **1998**, *177*, 347.
(6) Balzani, V.; Juris, A.; Venturi, M.; Campagna, S.; Serroni, S. *Chem. Rev.* **1996**, *96*, 759.
(7) Moyer, A. B.; Thompson, S. M.; Meyer, J. T. *J. Am. Chem. Soc.* **1980**, *102*, 2310−2312.
(8) Thompson, S. M.; Meyer, J. T. *J. Am. Chem. Soc.* **1981**, *103*, 5577−5579.
(9) Gersten, W. S.; Samuels, J. G.; Meyer, J. T. *J. Am. Chem. Soc.* **1982**, *104*, 4029−4030.
(10) Vining, J. W.; Meyer, J. T. *Inorg. Chem.* **1986**, *25*, 2023−2033.
(11) Meyer, J. T. *J. Electrochem. Soc.* **1984**, *131*, 221C.
(12) Sullivan, B. P.; Salmon, D. J.; Meyer, J. T. *Inorg. Chem.* **1978**, *17*, 3334−3341.
(13) Bruce, R. M. M.; Megebee, E.; Sullivan, B. P.; Thorp, H. H.; O'Toole, R. T.; Downard, A.; Pugh, J. R.; Meyer, J. T. *Inorg. Chem.* **1992**, *31*, 4864−4873.
(14) Gratzel, M. *Energy Resources Through Photochemistry and Catalysis*; Academic: New York, 1983.
(15) Tokel-Takvoryan, E. N.; Hemingway, E. R.; Bard, J. A. *J. Am. Chem. Soc.* **1973**, *95*, 6582−6589.
(16) Hartshorn, M. R.; Barton, K. J. *J. Am. Chem. Soc.* **1992**, *114*, 5919−5925.
(17) Sacksteder, L.; Lee, M.; Demas, J. N.; DeGraff, B. A. *J. Am. Chem. Soc.* **1993**, *115*, 8230−8238.
(18) Demadis, K. D.; Meyer, T. J.; White, P. S. *Inorg. Chem.* **1998**, *37*, 3610−3619.
(19) Basuli, F.; Peng, S. M.; Bhattacharya, S. *Polyhedron* **1998**, *17*, 2191−2197.
(20) Otsuka, T.; Takahashi, N.; Fujigasaki, N.; Sekine, A.; Ohashi, Y.; Kaizu, Y. *Inorg. Chem.* **1999**, *38*, 1340−1347.
(21) Constable, E. C.; Raithby, P. R.; Smit, D. N. *Polyhedron* **1989**, *8*, 367.
(22) Haga, M.; Isobe, K.; Boone, S. R.; Pierpont, C. G. *Inorg. Chem.* **1990**, *29*, 3795.

10.1021/om0303202 CCC: $25.00
Publication on Web 08/23/2003

two bpy ligands were retrieved from the Cambridge Structural Database,[28] i.e., (i) bis(2,2′-bpy)(salicylaldehydato)osmium perchlorate,[19] (ii) (3,5-di-*tert*-butylcatecholato-*O*,*O*′)bis(2,2′-bpy)osmium perchlorate,[22] and (iii) bis(2,2′-bpy)(catecholato-*O*,*O*′)osmium hexafluorophosphate.[23] In all these structures the coordination sphere of the Os atom is completed by a bidentate ligand and only one crystal structure[27] presents a monodentate ligand (a water molecule, together with a bidentate and a tridentate ligand), while none contain two monodentate ligands. Furthermore, to our knowledge, there are no structures for Os(bpy)$_2$ complexes containing carbon monoxide in the metal coordination sphere. For these reasons, we undertook a detailed investigation of two Os(bpy)$_2$ complexes, namely, [Os(bpy)$_2$(CO)Cl]PF$_6$ (**1**) and [Os(bpy)$_2$(CO)H]PF$_6$ (**2**).

The use of polypyridyl complexes as an important class of metallointercalators is well known.[29] A full assignment of the proton spectrum should be particularly useful for the correct location of metal complexes between stacked bases. 1D and 2D ^{1}H NMR experiments represent powerful tools for obtaining quick and essential information on the molecular structure and in evaluating the diastereoisomeric purity. However, the complete assignment of the polypyridine resonances remains extremely difficult,[30−35] and some ambiguities are still present in the literature data. Several partial assignments, based on previous experimental considerations, such as the proton chemical shift order of bipyridine rings in metal derivatives and the magnitude of the couplings, have been proposed.[33,35] In principle a full NMR assignment could be achieved by an array of NMR sequences (i.e., experiments such as HETCOR, HMBC, INADEQUATE, NOESY, etc.),[36] but these measurements cannot be successfully performed in all cases, because of the long experimental time and/or the low sample solubility. As recently shown by Reger et al. for the [*N*,*O*-PhC(O)(2-py)Ru(bpy)$_2$][PF$_6$] complex,[37] NMR data based on DQCOSY, gHMBC, and *J*-resolved experiments reduced the assignment ambiguities to a reasonable minimum. Still, a certain degree of indetermination remained even if the authors were able to suggest reasonable arguments based on the *trans* perturbation on the pyridyl moieties. We undertook an alternative approach by integrating theoretical and experimental results for the complete assignment of the ^{1}H NMR spectra and for the a priori elimination of any ambiguity. Density functional theory (DFT) calculations coupled with the gauge including atomic orbital (GIAO) calculations, as implemented in the Gaussian 98 set of programs,[38] were employed to help the full NMR assignment of the investigated complexes. Although the procedures for the calculation of the molecular properties responsible for the NMR spectra were discovered almost 40 years ago, only during recent years has this tool become available and popular, thanks to the solution of several practical computational problems. Actually, the first review on the subject appeared in the literature only a few years ago.[39]

The new generation of gradient-corrected DFT methods[40,41] such as Becke's three-parameter hybrid exchange potential (B3)[42] with the Lee−Yang−Parr (LYP),[43] Perdew (P86),[44] or Perdew−Wang (PW91)[45,46] correlation functionals are efficient and accurate computational methods, particularly for treating large systems carrying transition metals. Therefore, the DFT methods such as B3LYP and B3PW91 have became the dominant computational tools for dealing with complexes containing transition metal atoms.

A wide number of successful DFT calculations of NMR chemical shifts (δ), mainly on heteronuclei such as ^{13}C, ^{17}O, ^{29}Si, ^{31}P, or transition metal atoms,[47−53] have been carried out. These calculations have been used in the study of the three-dimensional structure of proteins,[54] for the identification of reactive cationic species in solution,[55] and to understand the relationships between structure and reactivity in organometallic catalysts.[56] Quantum mechanical calculations of ^{1}H chemical shifts

(23) Barthram, A. M.; Reeves, Z. R.; Jeffery, J. C.; Ward, M. D. *J. Chem. Soc., Dalton Trans.* **2000**, 3162.
(24) Shklover, V.; Zakeeruddin, S. M.; Nesper, R.; Fraser, D.; Gratzel, M. *Inorg. Chim. Acta* **1998**, *274*, 64.
(25) Basuli, F.; Peng, S. M.; Bhattacharya, S. *Polyhedron* **1999**, *18*, 391−402.
(26) Ashby, M. T. *J. Am. Oil Chem. Soc.* **1995**, *117*, 2000.
(27) Chien-Chung, C.; Goll, J. G.; Neyhart, G. A.; Welch, T. W.; Singh, P.; Thorp, H. H. *J. Am. Chem. Soc.* **1995**, *117*, 2970.
(28) Hallen, F. H. *Acta Crystallogr.* **2002**, *B58*, 380.
(29) Holmlin, R. E.; Dandliker, P. J.; Barton, K. J. *Angew. Chem., Int. Ed. Engl.* **1997**, *36*, 2714−2730.
(30) Steel, P. J.; Lahousse, F.; Lerner, D.; Marzin, C. *Inorg. Chem.* **1983**, *22*, 1488−1493.
(31) Bolger, J.; Gourdon, A.; Ishow, E.; Launay, J.-P. *Inorg. Chem.* **1996**, *35*, 2937−2944.
(32) Hage, R.; Haasnoot, G. J.; Reedijk, J.; Wang, R.; Vos, G. J. *Inorg. Chem.* **1991**, *30*, 3263−3269.
(33) Nieuwenhuis, A. H.; Haasnoot, G. J.; Hage, R.; Reedijk, J.; Snoeck, L. T.; Stufkens, J. D.; Vos, G. J. *Inorg. Chem.* **1991**, *30*, 48−54.
(34) Walsh, L. J.; Durham, B. *Inorg. Chem.* **1982**, *21*, 329−332.
(35) Baitalik, S.; Florke, U.; Nag, K. *Inorg. Chim. Acta* **2002**, *337*, 439−449.
(36) Braun, S.; Kalinowski, H.-O.; Berger, S. *150 and More Basic NMR Experiments: A Practical Course*; John Wiley & Son Ltd: New York, 1998.
(37) Reger, D. L.; Gardiner, J. R.; Smith, M. D.; Pellechia, P. J. *Inorg. Chem.* **2003**, *42*, 482.
(38) Frisch, M. J.; Trucks, G. W.; Schlegel, H. B.; Scuseria, G. E.; Robb, M. A.; Cheeseman, J. R.; Zakrzewski, V. G.; Montgomery, J. A. Jr.; Stratmann, R. E.; Burant, J. C.; Dapprich, S.; Millam, J. M.; Daniels, A. D.; Kudin, K. N.; Strain, M. C.; Farkas, O.; Tomasi, J.; Barone, V.; Cossi, M.; Cammi, R.; Mennucci, B.; Pomelli, C.; Adamo, C.; Clifford, S.; Ochterski, J.; Petersson, G. A.; Ayala, P. Y.; Cui, Q.; Morokuma, K.; Malick, D. K.; Rabuck, A. D.; Raghavachari, K.; Forestman, J. B.; Cioslowski, J.; Ortiz, J. V.; Baboul, A. G.; Stefanov, B. B.; Liu, G.; Liashenko, A.; Piskorz, P.; Komaromi, I.; Gomperts, R.; Martin, R. L.; Fox, D. J.; Keith, T.; Al-Laham, M. A.; Peng, C. Y.; Nanayakkara, A.; Challacombe, M.; Gill, P. M. W.; Johnson, B.; Chen, W.; Wong, M. W.; Andres, J. L.; Gonzales, C.; Head-Gordon, M.; Replogle, E. S.; Pople, J. A. *Gaussian 98* (revision A.9); Gaussian Inc.: Pittsburgh, PA, 1998.
(39) Helgaker, T.; Jaszunski, M.; Ruud, K. *Chem. Rev.* **1999**, *99*, 293−352.
(40) Ziegler, T. *Chem. Rev.* **1991**, *91*, 651.
(41) Parr, R. G.; Yang, W. *Density-Functional Theory of Atoms and Molecules*; Oxford University Press: Oxford, 1989.
(42) Becke, A. D. *J. Chem. Phys.* **1993**, *98*, 5648−5652.
(43) Lee, C.; Yang, W.; Parr, R. G. *Phys. Rev. B: Condens. Matter* **1988**, *37*, 785.
(44) Perdew, J. P. *Phys. Rev. B: Condens. Matter* **1986**, *33*, 8822.
(45) Perdew, J. P.; Wang, Y. *Phys. Rev. B: Condens. Matter* **1991**, *45*, 13244.
(46) Perdew, J. P.; Burke, K.; Wang, Y. *Phys. Rev. B: Condens. Matter* **1996**, *54*, 16533.
(47) Alkorta, I.; Elguero, J. *New J. Chem.* **1998**, 381.
(48) Dejaegere, A. P.; Case, D. A. *J. Chem. Phys. A* **1998**, *102*, 5280.
(49) Meine, T.; Goursot, A.; Seifert, G.; Weber, J. *J. Phys. Chem. A* **2001**, *105*, 620.
(50) Patchkovskii, S.; Ziegler, T. *J. Phys. Chem. A* **2002**, *106*, 1088.
(51) Bühl, M. *Organometallics* **1997**, *16*, 261.
(52) Bühl, M. *Chem. Phys. Lett.* **1997**, *267*, 251.
(53) Vivas-Reyes, R.; De Proft, F.; Biesemans, M.; Willem, R.; Geerling, P. *J. Phys. Chem. A* **2002**, *106*, 2753.
(54) de Dios, A. C.; Pearson, J. G.; Oldfiled, E. *Science* **1993**, *260*, 1491.
(55) Olah, A. G.; Shamma, T.; Burrichter, A.; Golam, R.; Prakash, G. K. S. *J. Am. Chem. Soc.* **1997**, *119*, 12923−12928.

are generally less accurate, because of the limited spectral width of the proton spectra. Chesnut[57] has shown that proton chemical shifts for small organic molecules can be obtained with 0.1 ppm accuracy adopting large basis sets and rotovibrational and correlation corrections.

Unfortunately such elaborate calculations are often impracticable for larger molecules, especially for transition metal complexes. The goal of the present study is to demonstrate that for these classes of molecules also calculations performed at much less demanding levels of theory, coupled with selected and easily available NMR experimental data, allow the complete assignment of the proton spectra, yielding a good agreement between the experimental and calculated sequences of chemical shift values.

Experimental Section

Reagents and Solvents. $(NH_4)_2OsCl_6$ was purchased from Avocado. 2,2′-bipyridine, obtained from Aldrich, was purified by crystallization from hexane and dried under vacuum over P_2O_5.[58] 1,2-Dimethoxyethane was purified by refluxing and distilling from sodium and benzophenone just before use. Neutral alumina for chromatography was obtained from Aldrich. All other reagents were of reagent grade and were used as received without any further purification.

$[Os(bpy)_2(CO)Cl]PF_6$ (**1**) and $[Os(bpy)_2(CO)(O_3SCF_3)](O_3SCF_3)$ (**3**) were prepared as previously reported.[59,60] $[Os(bpy)_2(CO)H]PF_6$ (**2**) was synthesized by refluxing an ethylene glycol solution of (**3**) (100 mg) under a nitrogen blanket for 1.5 h. The yellow color rapidly turned to purple. After cooling the solution to room temperature, 20 mL of aqueous NH_4PF_6 was added. A violet-red precipitate was collected and washed with water and diethyl ether.

X-ray Diffraction. The crystal structures of compounds **1** and **2** were solved by single-crystal X-ray diffraction analysis. Suitable crystals of **1** and **2** were obtained by slow evaporation of an acetonitrile/toluene mixture. Single-crystal diffraction data were collected at RT on a Bruker SMART-APEX CCD[61] area detector diffractometer, using graphite monochromatic Mo Kα (λ = 0.71073Å) radiation. Absorption correction was performed using SADABS.[62] The structure was solved by direct methods (SIR97)[63] and refined by full-matrix least-squares (SHELX97).[64] Hydrogen atoms (except for the hydride) were generated in calculated positions with XP[65] software. The hydride position was obtained from the analysis of the residual electron density after the location of all the other atoms and then refined by least squares. Since the refinement of the hydride position in **2** from X-ray diffraction data may be rather inaccurate, its correct position was obtained by theoretical calculations. We employed Jaguar[66] software, which is particularly suited for treating organometallic systems. A reliable model of the Os complex in the solid state was obtained by fixing the coordinates of the non hydrogen atoms to the values obtained from the X-ray analysis and optimizing the position of the hydride atom at the B3LYP[42,43] and local MP2[67−70] levels, employing the LAV3P[71,72] pseudopotential for Os and the 6-31G(d,p) basis set for the other atoms. The position of the hydride was then fixed in the X-ray data refinement to that obtained from the theoretical calculations. Graphical manipulations were carried out using XP[73] and MOLDRAW[74] software. The final atomic coordinates and temperature factors together with all other crystallographic information have been deposited.[75]

NMR Spectroscopy. The NMR spectra were recorded on JEOL EX 400 (B_0 = 9.4 T, ^{1}H operating frequency 399.78 MHz) and Bruker Avance 600 (B_0 = 14.1 T, ^{1}H operating frequency 600.13 MHz) spectrometers. Compound **1** was dissolved in deuterated acetonitrile, **2** in deuterated tetrahydrofuran, and **3** in deuterated dichloromethane. Chemical shifts were internally referenced relative to the residual protons in the employed deuterated solvents.

DQF-COSY experiments[76] were acquired using a JEOL EX 400. The number of data points in t_2 was 1024 for 256 t_1 values, with a pulse repetition of 3 s. 2D NOESY phase-sensitive experiments[77,78] were acquired using a Bruker Advance 600 by the States-TPPI method,[79] using 32K data points in t_2 for 256 t_1 values with a mixing time of 1 s. NMR simulations were performed with the software package gNMR,[80] version 4.1, adopting the full line shape iteration method, which is useful in determining strongly coupled systems such as ^{1}H spectra of mono- and disubstituted benzenes. For the simulation, the 16-proton spin system was divided appropriately in two parts, each containing two aromatic rings of the bipyridine groups; then the two-half spectra were joined together to get the complete spectrum.

Computational Details. The DFT method based on Becke's three-parameter hybrid functional[42] and Lee−Yang−Parr's[43] gradient-corrected correlation functional (B3LYP) was used. Geometries of **1**, **2**, and **3** were fully optimized in two steps using Gaussian 98.[38] During the first step we adopted the Los Alamos effective core potential double-ζ (LanL2Dz) for Os and the 3-21G basis sets for the other atoms. In the second step we raised the quality of the basis set of non-Os atoms to 6-31G(d). Calculations of the magnetic shielding σ were performed at the B3LYP/6-31++G(2d) level using the GIAO method of Gaussian98. The σ values were converted into proton chemical shifts δ, relative to the magnetic shielding of tetramethylsilane computed with the corresponding basis set. In the case of molecule **1**, using the Jaguar software we further improved the quality of the geometry used for the NMR

(56) Leitner, W.; Bühl, M.; Fornika, R.; Six, C.; Baumann, W.; Dinjus, E.; Kessler, M.; Krüger, C.; Rufinska, A. *Organometallics* **1999**, *18*, 1196.
(57) Chesnut, D. B. *Chem. Phys.* **1997**, *214*, 73.
(58) Amarengo, L. F.; Perrin, D. D. *Purification of Laboratory Chemicals*; Butterworth-Heinemann: Oxford, 1998.
(59) Kober, M. E.; Caspar, V. J.; Sullivan, B. P.; Meyer, J. T. *Inorg. Chem.* **1988**, *27*, 4587−4598.
(60) Sullivan, B. P.; Caspar, V. J.; Johnson, R. S.; Meyer, J. T. *Organometallics* **1984**, *3*, 1241−1251.
(61) *SMART*; Bruker AXS, Inc.: Madison, WI 53719, 1998.
(62) Sheldrick, G. M. *SADABS*. University of Göttingen: Germany, 1996.
(63) Altomare, A.; Burla, M. C.; Camalli, M.; Cascarano, G. L.; Giacovazzo, C.; Guagliardi, A.; Moliterni, A. G.; Polidori, G.; Spagna, R. *J. Appl. Crystallogr.* **1999**, *32*, 115.
(64) Sheldrick, G. M. *SHELXL-97*; University of Göttingen: Germany, 1997.
(65) *SHELXTL*; Bruker AXS, Inc.: Madison, WI 53719, 1998.
(66) *Jaguar 4.1*; Schrödinger Inc.: Portland, OR, 2000.
(67) Møller, C.; Plesset, M. S. *Phys. Rev.* **1934**, *46*, 618.
(68) Sæbø, S.; Pulay, P. *Theor. Chim. Acta* **1986**, *69*, 357.
(69) Sæbø, S.; Pulay, P. *Annu. Rev. Phys. Chem.* **1993**, *44*, 213.
(70) Sæbø, S.; Tong, W.; Pulay, P. *J. Phys. Chem.* **1993**, *98*, 2170.
(71) Hay, P. J.; Wadt, W. R. *J. Chem. Phys.* **1985**, *82*, 270.
(72) Hay, P. J.; Wadt, W. R. *J. Chem. Phys.* **1985**, *82*, 284.
(73) *SHELXTL*; Bruker AXS, Inc.: Madison, WI 53719, 1998.
(74) Ugliengo, P.; Viterbo, D.; Chiari, G. *Z. Kristallogr.* **1993**, *207*, 9−23.
(75) Supplementary information (coordinates of H atoms, anisotropic thermal parameters, bond distances and angles) has been deposited at the Cambridge Crystallographic Data Centre, with deposition numbers CCDC-208706 and CCDC-208707 for compounds **1** and **2**, respectively.
(76) Rance, M.; Sørensen, O. W.; Bodenhausen, G.; Wagner, G.; Ernst, R. R.; Wüthrich, K. *Biochem. Biophys. Res. Commun.* **1983**, *117*, 479.
(77) Jeener, J.; Meier, B. H.; Bachmann, P.; Ernst, R. R. *J. Chem. Phys.* **1979**, *69*, 4546.
(78) Wagner, G.; Wüthrich, K. *J. Mol. Biol.* **1982**, *155*, 347.
(79) Schorn, C. *NMR Spectroscopy: Data Acquisition*; Wiley-VCH: New York, 2001.
(80) Budzelaar, P. H. M. *gNMR* (4.1); Adept Scientific plc.: UK, 1999.

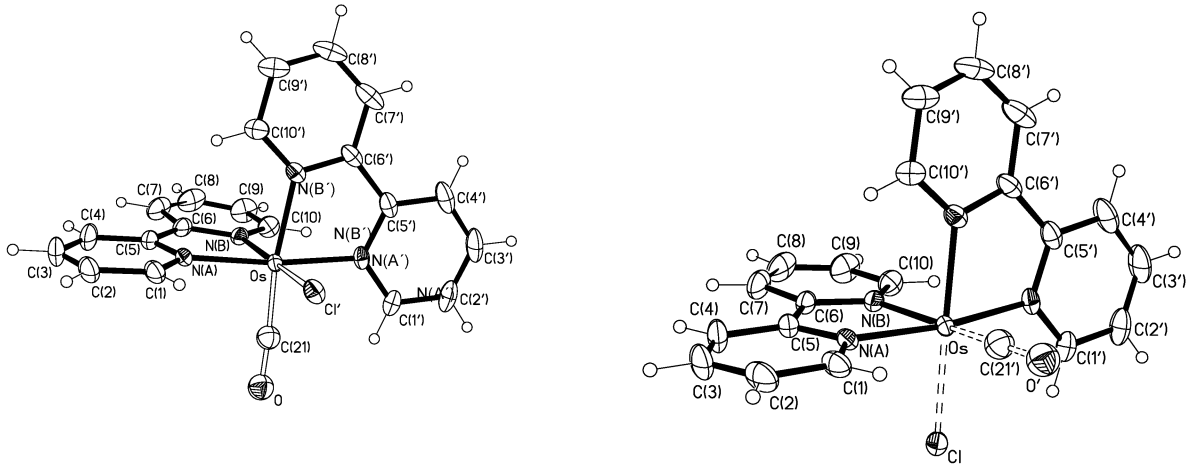

Figure 1. Drawing of the molecular structure of compound **1**, showing the adopted labeling scheme, with displacement ellipsoids drawn at the 20% probability level (the PF_6^- moiety is omitted for clarity). The two possible orientations of the [Os(bpy)$_2$(CO)(Cl)] complex in the crystal structure are shown in parts a and b, respectively (the asymmetric unit content has unprimed labels).

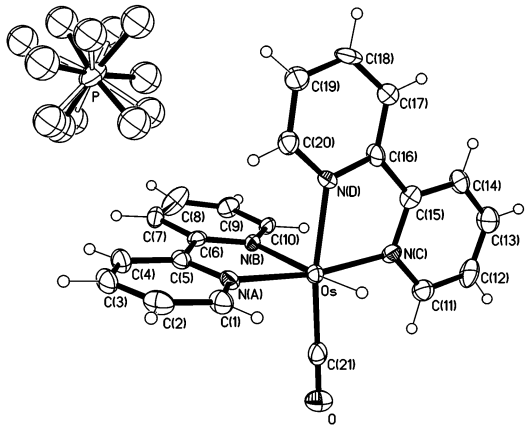

Figure 2. Drawing of the molecular structure of compound **2**, showing the adopted labeling scheme, with displacement ellipsoids drawn at the 20% probability level. The PF_6^- moiety is disordered, and the two possible positions are indicated by black and white bonds, respectively.

calculations: a full geometry optimization at the local MP2 level[67−70] with the LAV3P pseudopotentials for Os and the 6-31G(d, p) basis set for the other atoms was carried out in order to include the electron correlation effects. The L-MP2 optimized geometries were then employed to perform a new NMR calculation at the B3LYP/6-31++G(2d) level as described above.

Results and Discussions

Crystal Structures of 1 and 2. The X-ray structures of two osmium complexes of general formula *cis*-[Os(bpy)$_2$(CO)(Y)]$^+$, where Y = Cl^- (**1**) or H^- (**2**), were solved by single-crystal X-ray diffraction analysis (Figures 1 and 2). Crystallographic data and details of data collections and refinements are given in Table 1. For compound **3** (Y = $CF_3SO_3^-$) no suitable single crystals were obtained. Crystals of both **1** and **2** are racemic mixtures of the two optical isomers, and therefore they belong to centrosymmetric space groups. However, the arrangement of the two isomers in the crystal structures is very different. In complex **1**, the Cl^- and CO groups are characterized by static disorder, and the complexes are arranged so that two [Os(bpy)$_2$(CO)(Y)]$^+$ can occupy the same crystallographic position, assuming two orientations (depicted as separate moieties in Figure 1) related by a 2-fold rotation axis. In the crystal structure the asymmetric unit (unprimed labels in Figure 1) contains half molecule **1**, in which CO and Cl^- share the same orientation with a 50% occupancy factor. Despite the above-described disorder, the Cl^- and CO groups have been successfully located in the electron density after unconstrained X-ray data refinement. This

Table 1. Crystal Data for Complexes 1 and 2

	1	**2**
empirical formula	$C_{21}H_{16}ClF_6N_4OOsP$	$C_{21}H_{17}F_6N_4OOsP$
fw	711.00	676.56
temperature	293(2) K	293(2) K
wavelength	0.71073 Å	0.71069 Å
cryst syst	monoclinic	triclinic
space group	*C*2/*c*	$P\bar{1}$
unit cell dimens	a = 15.518(3) Å b = 13.419(3) Å c = 12.663(3) Å β = 111.07(3)°	a = 8.704(4) Å b = 9.959(4) Å c = 13.113(4) Å α = 91.90(4)° β = 97.53(4)° γ = 93.08(4)°
volume	2460.6(9) Å^3	1124.3(10) Å^3
Z	4	2
density (calcd)	1.919 Mg/m^3	2.034 Mg/m^3
abs coeff	5.42 mm^{-1}	5.54 mm^{-1}
F(000)	1360	648
cryst size (mm)	0.11 × 0.25 × 0.25	0.02 × 0.06 × 0.06
θ range for data collection	13.70 to 24.71°.	10.26 to 23.25°.
index ranges	$-18 \le h \le 18$, $-15 \le k \le 15$, $-14 \le l \le 14$	$-9 \le h \le 9$, $-11 \le k \le 11$, $-14 \le l \le 14$
no. of reflns collected	11 719	8218
no. of ind reflns	1715 [R(int) = 0.0329]	2667 [R(int) = 0.0420]
completeness to θ = 30.50°	82.0%	82.5%
refinement method	full-matrix least-squares on F^2	
no. of data/restraints/params	1715/0/164	2667/67/304
goodness-of-fit on F^2	1.007	1.014
final R indices [$I>2\sigma(I)$]	R1 = 0.0270, wR_2 = 0.0634	R1 = 0.0769, wR_2 = 0.1855
R indices (all data)	R1 = 0.0302, wR_2 = 0.0645	R1 = 0.0686, wR_2 = 0.1785
largest diff peak and hole	0.93 and −1.30 e Å^{-3}	1.18 and −2.81 e Å^{-3}

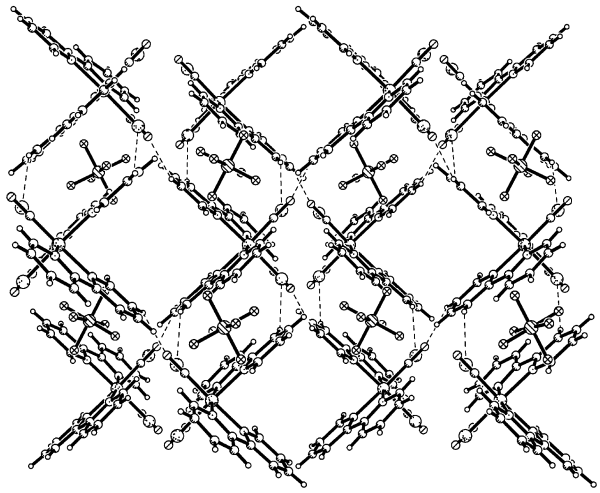

Figure 3. Crystal packing of compound **2**. Dotted lines indicate the C−H···Y (Y = CO or Cl^-) contacts between the $[Os(bpy)_2(CO)(Cl)]^+$ moieties.

kind of disorder may be possible because of the similarity of the CO and Cl^- groups, which have similar shape, vdW dimensions, and hydrogen bonding affinity. Therefore **1**, which has a C_1 molecular symmetry, from the point of view of the real electron density, can be considered as a pseudo-C_2 molecule. As a result, the molecules can be arranged in the centrosymmetric monoclinic *C*2/*c* space group, with the 2-fold rotation axis relating two half-molecules. It is worth noting that also bis(bpy)(catecholato-*O*,*O*′)osmium),[23] which is a C_2 molecule, crystallizes in the *C*2/*c* space group, and this represents the only other case with such a symmetry among the osmium polypyridine complexes retrieved from the Cambridge Structural Database.[28]

The crystal packing of compound **1** is driven by the ionic forces between the positive Os-containing moiety and the negative PF_6^- anions, which are disposed in an alternate way, as shown in Figure 3. In addition, interactions between the C−H groups of the bipyridyl moieties and the possible hydrogen bond acceptors among the ligands bound to Os (CO and Cl^-) are present. Different opinions on the nature and name[81−83] of these weak interactions (hydrogen bond, anti-hydrogen bond, vdW interactions, etc.) can be found in the literature. The only definitive conclusion is that these types of interactions are very weak but are still stabilizing contacts, and they are the only possible ones in this kind of compound.

In complex **2** (Figure 2), the two monodentate ligands (CO and hydride) are rather different, and the molecules do not show the pseudo C_2 symmetry observed in **1**, and can therefore assume only one orientation in any given crystallographic position. The asymmetric unit contains one complete $[Os(bpy)_2(CO)(H)][(PF_6)]$ (**2**) moiety, and the molecules can be arranged in the triclinic $P\bar{1}$ space group, with the two isomers related by the inversion center. Nevertheless, a certain degree of disorder is also present in compound **2**, since the fluorine atoms in the PF_6^- fragment cannot be well located. The electron density could be successfully interpreted assuming two possible orientations (indicated in Figure 2 by black and white bonds) for the PF_6^- group. This disorder is probably due to the high symmetry of the PF_6^- fragment and to the nondirectional ionic forces, which link the PF_6^- anion to the organometallic fragment. The crystal packing of compound **2** is characterized by the same features of compound **1**, with some weak interactions between the C−H groups and the monodentate ligands.

To obtain more accurate hydrogen atom positions, an ab initio geometry optimization was carried out, employing the Jaguar software, fixing the coordinates of all heavier atoms, well located by the X-ray analysis. In this way reliable models of the molecular structures of complexes **1** and **2** in the solid state were obtained. As expected, only the position of the hydride atom changed significantly, as summarized in Table 2. The different employed levels of theory (DFT and local MP2) do not give significant differences in the hydride location. Then, as described in the next section, full geometry optimizations of compounds **1** and **2** were carried out to obtain minimum energy (gas phase) geometries suitable for simulating the NMR spectra.

NMR Experiments and DFT Calculations. We have successfully carried out the assignment of the ^1H NMR spectra of the title compounds using a combination of proton 1D and 2D NMR spectroscopic techniques together with the use of DFT calculations for the isolated molecule. In Figure 4 the structural representation and the adopted proton numbering scheme for **1**, **2**, and **3** are reported. The ^1H spectrum of **1** shows 16 separate resonances, distributed in a small chemical shift range (Table 3) since the bpy spin systems are almost isochronous. As previously mentioned, it is therefore difficult to find a practical and unquestionable set of experiments for the complete assignment of the proton peaks to the A, B, C, or D ring. The calculated NMR spectra have been a good starting point for the full comprehension of the experimental NMR analysis. In complex **1**, one would hope to initiate the NMR labeling process from the most informative resonances, i.e., the lowest field doublets at δ 9.71 and 9.35 respectively, which appear to be well separated from the other peaks. Unfortunately doublets are expected for the H_1, H_4, H_5, H_8, H_9, H_{12}, H_{13}, and H_{16} protons, and it is rather difficult to discriminate among them, because of the well-known different and variable behavior of polypyridyl ligands in metal transition complexes. These facts prompted us to try to predict the absolute chemical shift values by the use of DFT calculations (for details of these calculations see the Experimental Section) and to exploit them for a full comprehension of the spectrum. NMR spectra were calculated, always at the B3LYP/6-31++G(2d) level, on the geometry obtained after B3LYP/3-21G and B3LYP/6-31G(d,p) full geometry optimization to understand the minimum level of calculation required for reliable calculated NMR spectra. In addition, to check the utility of a higher level of calculation, we also performed, in the case of **1**, an NMR calculation at the usual B3LYP/6-31++G(2d) level, employing the geometry obtained after a full geometry optimization at the local-MP2/6-31G(d,p)[67−70] level. The main geometric features of compounds **1**, **2**, and **3** are reported in Table 2. From the geometrical point of view, the different levels of calculation employed for the

(81) Aime, S.; Diana, E.; Gobetto, R.; Milanesio, M.; Valls, E.; Viterbo, D. *Organometallics* **2002**, *21*, 50.
(82) Orlova, G.; Sheiner, S. *J. Phys. Chem. A* **1998**, *102*, 260−269.
(83) Sheiner, S.; Kar, T. J. *J. Phys. Chem. A* **2002**, *106*, 1784−1789.

Table 2. Selected Bond Lengths (Å) and Angles (deg) for Complexes 1, 2, and 3: Comparison between the DFT Calculations and X-ray Structures

		Os−N(A)	Os−N(B)	Os−N(C)	Os−N(D)	Os−C	Os−Y	C−Os−H
1	X-ray	2.066(3)	2.083(4)	2.066(3)	2.083(4)	1.79(2)	2.322(6)	
	B3LYP/3-21G	2.093	2.092	2.074	2.129	1.892	2.484	
	B3LYP/6-31G(d)	2.114	2.106	2.092	2.166	1.877	2.447	
	L-MP2/6-31G(d,p)	2.192	2.210	2.196	2.284	1.895	2.506	
2	X-ray	2.069(1)	2.162(1)	2.007(1)	2.154(1)	1.86(3)	2.06(3)[a]	94.0(1)
							1.68(3)[b]	
	B3LYP/6-31G(d,p)[c]						1.672	87.3
	L-MP2/6-31G(d,p)[c]						1.668	88.7
	B3LYP/3-21G[d]	2.092	2.185	2.067	2.132	1.885	1.650	86.7
	B3LYP/6-31G(d)[d]	2.111	2.221	2.085	2.162	1.870	1.648	87.2
3	B3LYP/3-21G	2.099	2.090	2.110	2.170	1.884	2.124	
	B3LYP/6-31G(d)	2.096	2.090	2.106	2.167	1.885	2.122	

[a] After X-ray data refinement without restraint on the hydride position. [b] After X-ray data refinement imposing restraints on the Os−H bond distance and C−Os−H angle according to the values obtained by theoretical calculations. [c] Jaguar calculation with all non hydrogen atom positions fixed as in the crystal structure after X-ray refinement. [d] Gaussian98 calculation with complete geometry optimization.

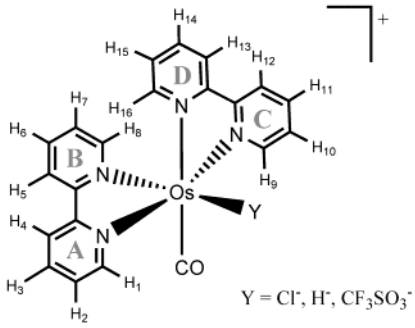

Figure 4. Schematic representation of the complexes of general formula [Os(bpy)$_2$(CO)(Y)]$^+$ with the adopted hydrogen atom labeling.

geometry optimization give similar results, even if some differences among the calculated structures and with respect to the X-ray structure arise. All the calculated Os−N, Os−C, and Os−Y distances (see Table 2) are larger than in the crystal structure, and the overestimation increases as the level of the calculation increases. The Os−H value after X-ray data refinement of compound **2** is largely overestimated (∼0.3 Å), while theoretical calculations give a value in keeping with that from neutron diffraction, as we already observed in a previous work.[81] Two other smaller but significant discrepancies (∼0.15 Å) occur in the C−Os and Cl−Os distances in **1**, where the CO and Cl$^-$ location in the X-ray crystal structures is affected by the disorder of these two ligands.

From the DFT calculations it is clear that the two highest frequencies must be associated with the H_1 and H_9 protons of the A- and D-pyridine rings, respectively. The resonances associated with each of the four pyridyl spin systems are then identified by DQF-COSY, and the DFT data were also useful in solving doubts about overlapped signals during the assignment work. Calculated and experimental ^{1}H chemical shifts are reported in Table 3. This mixed approach allowed the complete proton labeling of all the aromatic peaks (see Figure 5). In the case of compound **2** the same approach has been used. From the DFT calculations the two highest frequencies were again associated with the H_1 and H_9 protons. Unfortunately, in the experimental ^{1}H spectrum recorded in deuterated tetrahydrofuran, these two peaks are isochronous. The presence of the hydride ligand in complex **2** prompted us to perform a ^{1}H−^{1}H NOESY phase-sensitive experiment. From the cross-peak between the hydride and the overlapped signals of H_1 and H_9, shown in Figure 6, a first confirmation of the accuracy of the DFT calculations was obtained. Then the assignment ambiguities, due to this overlap, were overcome by adding 0.1 mL of C_6D_6 to the tetrahydrofuran solution. For the well-known ASIS effect[84−86] (aromatic solvent-induced shift) we were able to differentiate the two resonances. A new ^{1}H−^{1}H NOESY phase-sensitive experiment was carried out, and the cross-peaks between H_1 and the hydride hydrogen (Figure 7) was found and then by proceeding via the other cross-peaks the complete assignment was obtained. The computed hydride chemical shifts are −4.91 and −5.43 ppm for the geometry optimizations with the 3-21G or the 6-31G(d) basis sets, respectively, while the experimental one is −11.4 ppm. The error is relatively large, probably due to the motion of the hydride. Moreover, the relativistic effects become non-negligible in the presence of a heavy atom like osmium. This has been confirmed by Ziegler and co-workers,[87] who analyzed the factors responsible for the observed hydridic ^{1}H NMR shift.

Furthermore, we solved the ^{1}H spectrum of complex [Os(bpy)$_2$(CO)(CF$_3$SO$_3$)]$^+$ (**3**) with the same approach described above. The results confirm that the downfield resonances are again associated with protons in the A- and C-pyridine rings, but now the order is different with H_9 at 9.49 ppm and H_1 at 9.12 ppm. In this case the computing time was noticeably higher than for **1** and **2**. A more diffuse basis set ought to be employed, but, even so, more reliable results cannot be obtained due to rotovibrational and solvent effects.[39] Unfortunately, with the currently available hardware and software resources, such accurate calculations can be applied only to small molecules, with no more than 10−15 atoms and not containing heavy atoms such as Os. Looking at Table 3, it can be seen that the main deviations between calculated and experimental chemical shifts can be easily rationalized, noting that the NMR calculations on the 6-31G(d) geometry (i) overestimate the chemical shifts of H_1, H_8, and H_9 (with the unique exception of

(84) Lazlo, P. *Prog. NMR Spectrosc.* **1967**, *3*, 231.
(85) Ronayne, J.; Williams, D. H. *Annu. Rep. NMR Spectrosc.* **1969**, *2*, 83.
(86) Rummens, F. H. A.; Krystynak, R. H. *J. Am. Chem. Soc.* **1972**, *94*, 6914.
(87) Ruiz-Morales, Y.; Schreckenbach, G.; Ziegler, T. *Organometallics* **1996**, *15*, 3920.

Table 3. Experimental and Calculated Chemical Shift Values for Complexes 1, 2, and 3

δ of complex 1 (ppm)					δ of complex 2 (ppm)				δ of complex 3 (ppm)			
		calc[a]				calc[a]			calc[a]			
exptl		B3LYP/ 3-21G	B3LYP/ 6-31G(d)	MP2/ 6-31G(d,p)	exptl		B3LYP/ 3-21G	B3LYP/ 6-31G(d)	exptl		B3LYP/ 3-21G	B3LYP/ 6-31G(d)
H_1	9.71	10.61	10.31	10.07	H_1	9.44	9.88	9.80	H_9	9.49	10.49	10.00
H_9	9.35	9.67	9.66	9.64	H_9	9.44	9.52	9.41	H_1	9.12	10.16	9.75
H_4	8.52	8.16	8.24	8.20	H_4	8.69	8.29	8.25	H_4	8.65	8.71	8.42
H_{13}	8.49	8.11	8.20	8.12	H_5	8.59	8.22	8.19	H_5	8.48	8.66	8.27
H_{12}	8.44	8.17	8.25	8.22	H_{13}	8.54	8.03	8.05	H_{12}	8.45	8.82	8.06
H_5	8.38	7.96	8.05	8.04	H_{12}	8.50	8.07	8.08	H_{13}	8.42	8.78	8.13
H_3	8.32	8.24	8.31	8.31	H_3	8.26	8.17	8.19	H_3	8.37	8.76	8.40
H_{14}	8.07	7.95	7.97	8.11	H_6	8.05	7.92	7.98	H_{14}	8.13	8.53	8.04
H_{11}	8.04	8.02	8.07	8.16	H_{14}	8.01	7.83	7.88	H_{11}	8.08	8.67	8.18
H_6	7.99	7.85	7.90	8.01	H_{11}	7.89	7.82	7.89	H_6	8.01	8.39	8.00
H_8	7.96	7.90	8.08	8.15	H_{16}	7.78	7.68	7.68	H_2	7.89	8.42	8.00
H_2	7.86	7.78	7.85	7.81	H_2	7.61	7.67	7.66	H_8	7.77	8.52	8.04
H_{10}	7.68	7.66	7.62	7.60	H_{10}	7.43	7.40	7.41	H_{10}	7.72	8.40	7.84
H_{15}	7.39	7.24	7.21	7.28	H_{15}	7.40	7.09	7.14	H_{15}	7.51	7.79	7.25
H_{16}	7.26	7.45	7.45	7.93	H_7	7.39	7.21	7.28	H_{16}	7.30	7.97	7.32
H_7	7.26	7.17	7.15	7.18	H_8	7.35	7.63	7.71	H_7	7.30	7.81	7.20

[a] Geometry optimization level of calculation is reported; NMR calculation has been performed at B3LYP/6-31++G(2d).

Table 4. Intercept (*A*), Slope (*B*), Regression Coefficient (*r*), and Standard Deviation (SD) of the Linear Regression between Experimental and Calculated Chemical Shift Values for Complexes 1, 2, and 3 According to the Equation Calc = (*A* + *B*) Expt

	geom opt	*A*	*B*	*r*	SD
1	B3LYP/3-21G	−1.79 ± 0.92	1.21 ± 0.11	0.945	0.293
	B3LYP/6-31G(d)	−1.31 ± 0.70	1.15 ± 0.09	0.964	0.224
	L-MP2/6-31G(d, p)	−0.0821 ± 0.90	1.01 ± 0.11	0.926	0.286
2	B3LYP/3-21G	−0.31 ± 0.82	1.02 ± 0.10	0.938	0.265
	B3LYP/6-31G(d)	0.24 ± 0.80	0.96 ± 0.10	0.933	0.259
3	B3LYP/3-21G	−0.34 ± 0.94	1.10 ± 0.11	0.932	0.271
	B3LYP/6-31G(d)	−1.40 ± 0.93	1.17 ± 0.11	0.940	0.270

H_9 in **2**), which are close to the CO and Y ligands, and (ii) underestimate the chemical shifts of H_4, H_5, H_{12}, and H_{13}, which are characterized by short H···H contacts (H_{12}···H_{13} and H_{12}···H_{13} contacts are in the range 2.18(1)−2.24(1) Å in crystal structures of **1** and **2**). The eight other hydrogen atoms present deviations smaller than 0.1 ppm, except for H_{15} in compounds **2** and **3**, which shows an unexpected large error (see Table 3). Since we get absolute values, the criteria to evaluate the quality of the calculations should be the closeness of the slope to 1 and the intercept to 0 rather than the correlation coefficient *r*. Rablen and co-workers[88] compared different DFT methods for the estimation of ^{1}H δ of small to medium sized molecules. They found that the best compromise between quality and computational cost is represented by the 6-31G(d, p)//6-311G++(d,p) level of calculation (with this notation we mean the basis set used for geometry optimization//NMR calculation), instead of our 3-21G or 6-31G(d)//6-31G++(2d). At this level the quality of the results is certainly inferior to that previously found by several authors for simpler organic systems;[47,57] however we have shown that this approach can still be used to achieve a reasonable and accurate NMR assignment if the calculations can be carried out in limited CPU times and with almost standard computing capabilities.

NMR simulations have also been performed to obtain *J*-coupling information for all the aromatic resonances and to check the agreement with the experimental data.[89]

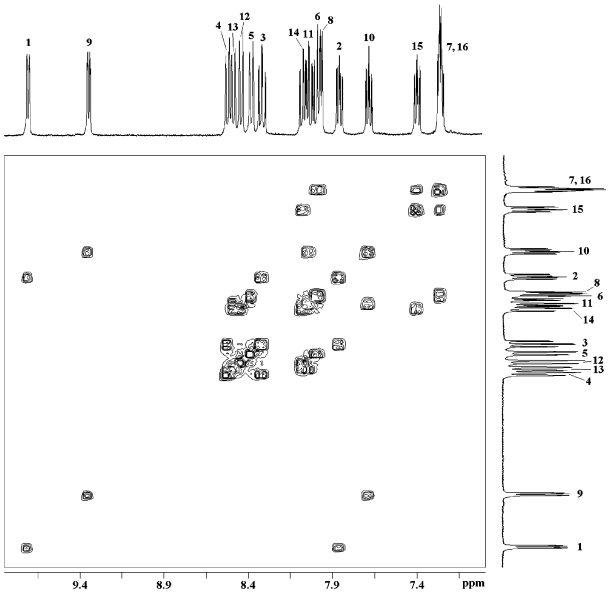

Figure 5. 400 MHz ^{1}H−^{1}H COSY NMR spectrum of $[Os(bpy)_2(CO)(Cl)]PF_6$ in deuterated acetonitrile.

Conclusions

The crystal structures of $[Os(bpy)_2(CO)(Cl)][(PF_6)]$ (**1**) and $[Os(bpy)_2(CO)(H)][(PF_6)]$ (**2**) represent the starting point for the theoretical calculations employed for the precise location of all the hydrogen atoms in the solid state and for the interpretation of the NMR data in solution. Furthermore, theoretical calculations allowed us to obtain a model of the structure of compound $[Os(bpy)_2(CO)(CF_3SO_3)][(CF_3SO_3)]$ (**3**), for which no suitable crystal was obtained. X-ray data indicated that in compound **1** the CO and Cl^- ligands can occupy the same crystallographic positions, thanks to their similarity in hydrogen bond affinity, vdW dimension, and shape. On the other hand, in compound **2**, where the two monodentate ligands (H and CO) on the Os atom

(88) Rablen, P. R.; Pearlman, S. A.; Finkbiner, J. *J. Phys. Chem. A* **1999**, *103*, 7357−7363.

(89) NMR simulation and *J* coupling values for **1**, **2**, and **3** are reported in the Supporting Information.

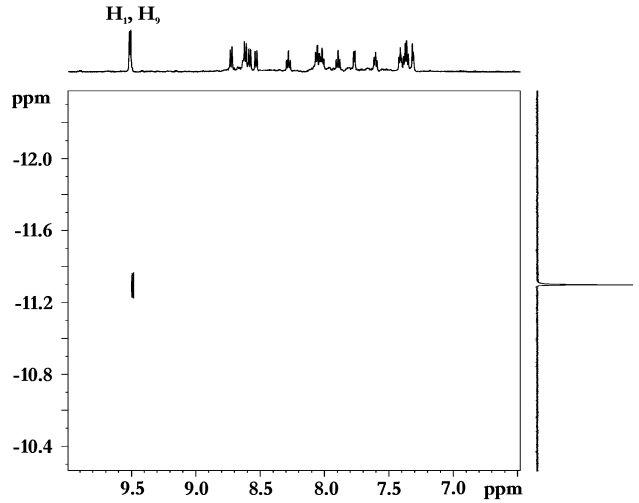

Figure 6. 600 MHz ^{1}H−^{1}H NOESY phase-sensitive NMR spectrum of [Os(bpy)$_2$(CO)(H)]PF$_6$ in deuterated tetrahydrofuran.

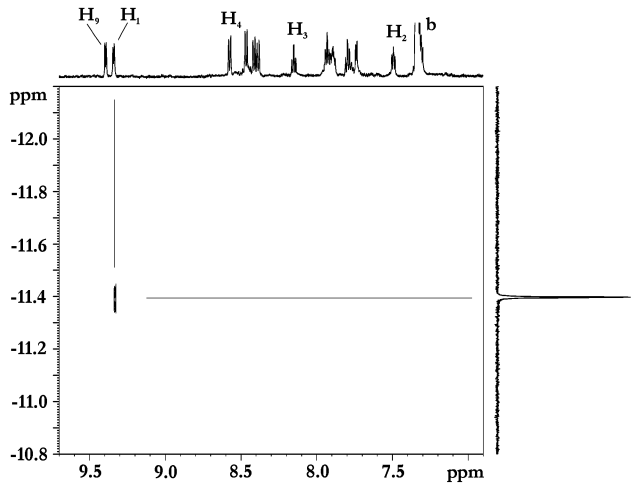

Figure 7. 600 MHz ^{1}H−^{1}H NOESY phase-sensitive NMR spectrum of [Os(bpy)$_2$(CO)(H)]PF$_6$ in deuterated tetrahydrofuran with 0.1 mL of deuterated benzene. The peak labeled with b is benzene.

have different geometry and bonding features, no disorder was observed in the structure of the [Os(bpy)$_2$(CO)(H)] moiety. Theoretical calculations enabled us at first to achieve an accurate model of the structures of **1** and **2** in the solid state and in solution. To solve the difficulties in the assignment of the proton NMR spectra of complexes **1**, **2**, and **3** we had fundamental help from the DFT calculations. All the proton resonances have been assigned using a simple ^{1}H−^{1}H DQF COSY spectrum and the calculated magnetic shielding constants obtained as described above. Correspondence between experimental and theoretical magnetic shielding constants could not always be achieved, because of the small chemical shift range and because we did not take into account the rotovibrational and solvent effects. Nevertheless, it is rather important to note that the trends of the resonances in the aromatic region show a good correspondence between the theoretical and the experimental data in all three compounds and for all geometry optimization levels. Indeed the assignment could be confirmed by the relatively low level of calculation employed, and in the case of **2** also by NOESY data. To get a better agreement between experimental and theoretical data, it would be necessary to evaluate the NMR shielding tensor with a basis set larger than 6-31++G(2d), but this would require unfeasibly long computing times. The geometry optimization level of calculation does not seem to be so critical for our purpose. Furthermore, efforts to get higher and higher basis sets for theoretical calculations could be useless unless rotovibrational and solvent effects are taken into account. That is particularly true in the case of ^{1}H NMR because of the limited spectral width of the proton spectra.

Acknowledgment. The authors thank Prof. D. Viterbo (Università del Piemonte Orientale) for useful discussions.

Supporting Information Available: ^{1}H−^{1}H COSY spectra and ^{1}H NMR simulations for **1**, **2**, and **3** and coupling constant tables for **1**, **2**, and **3**. This material is available free of charge via the Internet at http://pubs.acs.org.

OM0303202